Polymer Bulletin (2024) 81:10631–10644
https://doi.org/10.1007/s00289-024-05171-7

ORIGINAL PAPER

Strain rate sensitive polyampholyte hydrogels via well-dispersed XLG sheets

Esra Su[1] · **Gaukhargul Yelemessova**[2] · **Gaukhar Toleutay**[2,3]

Received: 7 November 2023 / Revised: 23 January 2024 / Accepted: 24 January 2024 /
Published online: 11 March 2024

Abstract

The physical interactions between anionic and cationic monomers and the layered silicate clay mineral Laponite (XLG) have received great attention because of their potential for a variety of applications such as strain sensitive sensors, wearable electronics, drug delivery systems, and tissue engineering applications. A detailed investigation of the interaction between XLG and charged monomers is presented in this article. The study includes the observation of the changes in the viscosity of the solutions and the mechanical performance of the gels at various concentrations by adding XLG to the ionic monomer solution. The ionic interactions between XLG and the charged monomers, driven by electrostatic forces, play a crucial role in gelation and formation of a three-dimensional network, giving the structure strain rate sensitivity. In this way, the addition of XLG nanoparticles not only improves the mechanical properties of the gels, but also gives us information about the microstructure of the mechanical properties that change depending on the strain rate.

Keywords Physical interactions · XLG nanoparticles · Polyampholyte hydrogels · Viscosity · Mechanical performance · Strain rate

✉ Esra Su
esra.su@istanbul.edu.tr

✉ Gaukhar Toleutay
gtoleuta@utk.edu

[1] Department of Aquatic Biotechnology and Genomics, Faculty of Aquatic Sciences, Istanbul University, 34134 Istanbul, Turkey

[2] Laboratory of Engineering Profile, Satbayev University, 050013 Almaty, Kazakhstan

[3] Department of Chemistry, University of Tennessee, Knoxville, TN 37996, USA

Introduction

For tough hydrogels with high mechanical strength, the energy distribution mechanism during deformation is crucial. This energy distribution mechanism can be achieved by incorporating reversible crosslinks such as hydrogen bonds and electrostatic and hydrophobic interactions under deformation. Depending on the strain rate, these reversible bonds can be broken and re-formed under deformation, resulting in different mechanical properties. Increased strain rate causes the crosslinks to break quickly, whereas the extended deformation times delay crosslink breakage, resulting in tougher and more ductile material. The mechanical properties of the polymer materials can be improved or easier production and processing steps can be developed by illuminating the change in the microstructure of the materials dependent on the strain rate. In order to better understand the structure of tough hydrogels with reversible crosslinks, it is important to examine the strain rate-dependent mechanical properties. Herein, we prepared nanocomposites with high strain rate sensitivity by incorporating Laponite (XLG) sheets to the structure of polyampholyte hydrogels associated with electrostatic interactions. XLG is a member of the smectite family, which consists of a silicate layer sandwiched between two layers of magnesium or lithium ions [10, 11]. Thanks to this unique structure, XLG can form stable colloidal suspensions in water, exhibiting a gel-like behavior and thixotropic characteristics associated with exceptional swelling capacity and stability. It also finds extensive use as a rheology modifier, stabilizer, and thickening agent in industries such as cosmetics, paints, pharmaceuticals, and ceramics [1, 2, 4, 8, 13, 18] and serves as a reinforcing agent in polymer nanocomposites, improving their mechanical properties and dimensional stability.

Poly(2-Acrylamido-2-methylpropane sulfonic acid) (PAMPS) and poly([3-(Methacryloylamino)propyl]trimethylammonium chloride) (PMAPTAC)-based polyampholyte hydrogel contains a high percentage of ionic bonds as well as conventional chemical crosslinks. The reversible bonds between the anionic and cationic polymer units as well as the positive (+) and negative charges (−) on the lateral and top surfaces of XLG, respectively, give the material high strain rate sensitivity. Meanwhile, AMPS is an important monomer in the field of polymer chemistry. Its hydrophilicity and reactivity granted by the sulfonic acid functionality [3, 12, 14, 15, 25–27, 30] make it ideal for copolymerization and modification of various polymers. For example, AMPS monomer is widely used in the development of superabsorbent polymers which are often explored [20, 22–24], in biomedical, tissue engineering, and agricultural applications as well as in the development of flocculants and dispersants for water treatment processes. Furthermore, AMPS-based polymers have been used in enhanced oil recovery, textiles, and adhesives [6, 7, 9, 17, 28, 29].

When XLG and AMPS are combined in an aqueous system, fascinating physical interactions occur, leading to the formation of gel-like structures in which the layered structure of XLG provides a high surface area for AMPS monomers to interact and adsorb onto the clay surface. Meanwhile, the sulfonic acid groups

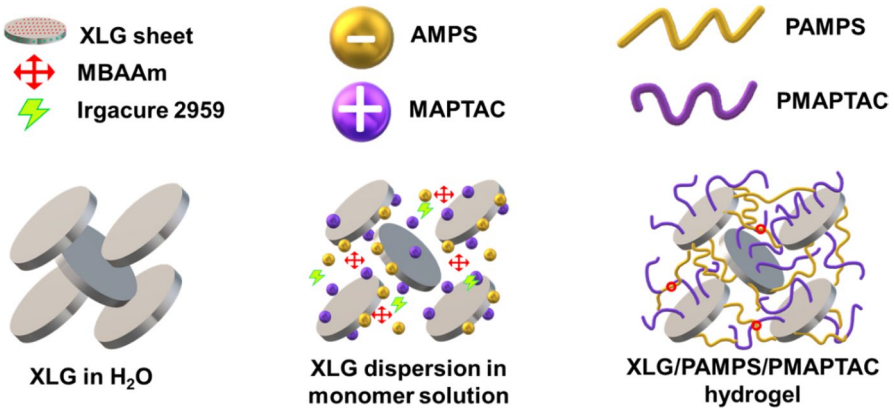

Scheme 1 Representation of the XLG dispersions in distilled water, monomer (AMPS+MAPTAC) solutions, and hydrogel

in AMPS can form electrostatic interactions with the charged surface of XLG, resulting in a three-dimensional network with enhanced mechanical properties (strength, stiffness, and dimensional stability) [2, 5, 22] and improved interfacial adhesion [12, 14]. These properties allow for applications related to gas and liquids permeability, packaging, drug release, and others [16, 21, 24, 29]. From a rheology point of view, the XLG/AMPS structures exhibit thixotropic behavior, whose viscosity decreases under shear stress and recovers once the stress is removed.

While the potential applications and properties of XLG/AMPS hydrogels are appealing, there is still little fundamental understanding of these systems. For example, Su and Okay [22] synthesized chemically crosslinked XLG/AMPS hydrogels and reported that the incorporation of the chemical permanent bonds weakens hydrogen bonding interactions. However, in combination, the different interactions create water soluble and tough materials [2, 23]. Following these discussions, in this article we investigated the physical interactions between XLG and AMPS, highlighting the synergistic effects and their implications for advanced applications for understanding the underlying mechanisms, and tailoring their interactions. As a result of our study, we observed a drastic change in the physical behavior of XLG and AMPS. The viscosity of AMPS/XLG gels was decreased under shear stress with increasing XLG content in the system. Additionally, the mechanical properties of the hydrogels are enhanced by the incorporation of XLG nanoparticles. A higher XLG content in the system reinforces the mechanical strength, stiffness, and dimensional stability of the gels.

Here, we synthesized hydrogels with XLG sheets dispersed in solution containing equal amounts of anionic (AMPS) and cationic monomers (MAPTAC), and we obtained both high mechanical strength and examined the dependence of mechanical properties on strain rate (Scheme 1). Within the scope of the study, mechanical parameters of the synthesized materials such as modulus, rupture

stress and strain were investigated for the compression tests, both after synthesis and in the water-swelling equilibrium.

Results and discussion

Binary systems

In this study the synthesis of XLG/AMPS hydrogels involved the combination of XLG nanoparticles with AMPS monomers and subsequent crosslinking to form a stable gel network. XLG nanoparticles act as a reinforcing agent, while AMPS monomers contribute to the hydrophilicity and reactivity of the hydrogel. Various methods can be employed for the synthesis of XLG/AMPS hydrogels, including free radical polymerization, in situ gelation, and self-assembly approaches. We particularly used the free radical method of polymerization to control the rheological and mechanical properties of the gels, such as gelation time, mechanical strength, and swelling behavior, by adjusting the concentrations of XLG and AMPS monomer.

XLG systems without AMPS monomers were investigated in the first series to examine how ionic interactions affect rheology. The viscoelastic properties of the system were studied by changing the ratio of XLG gels. Increased concentrations of XLG in the system result in a rise in ionic interactions, causing the system to be more elastic (Fig. 1). The results of the study showed that the viscosity increased with the same way when the ratio of XLG gels increased. XLG had a limit of 0.1 g mL^{-1} in the system due to precipitation, which causes it to become viscous, while 0.01–0.05 is sufficient. Our current work focuses on its ionic structure and interactions. We aim to understand how the polymer behaves in response to changes

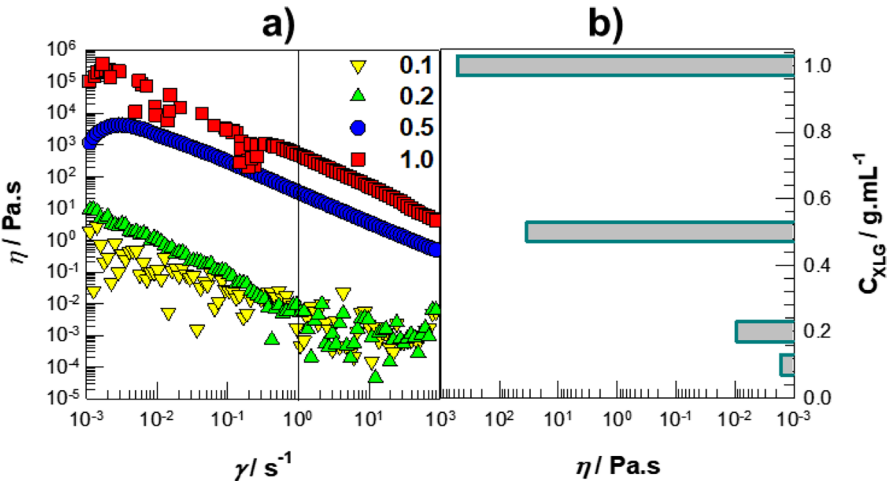

Fig. 1 **a** Viscosity (η) of XLG dispersions in distilled water depending on strain rate. **b** Viscosity values η of XLG dispersions depending on XLG amount at 1 s^{-1}. The amount of XLG dissolved in 10 mL of water is shown on the graph

in ionic strength. In addition, we are looking into the role of the ionic structure in the mechanical and rheological properties of gels.

The rheological properties of XLG/AMPS hydrogels were explored by focusing on their viscoelastic behavior and shear-thinning characteristics. XLG/AMPS hydrogels exhibit unique viscoelastic behavior, meaning they possess both viscous (liquid-like) and elastic (solid-like) characteristics. This behavior is a result of the interactions between the XLG nanoparticles, AMPS monomers in a polymer network.

During the incorporation of AMPS into the XLG system, the hydrogels exhibited predominantly elastic behavior, characterized by the ability to store, and recover energy. This elastic response arises from the physical entanglements between the polymer chains and the reinforcement provided by the Laponite nanoparticles. As a result, these hydrogels display excellent shape recovery and resistance to deformation. The viscoelastic behavior of the polymers was not affected by increased concentrations of XLG in the AMPS/XLG system, which is an excellent result (Fig. 2). This indicates that XLG does not interact with the polymer molecules in a significant manner. Furthermore, it suggests that the viscoelastic properties of the polymer remain unchanged even at high XLG concentrations (Fig. 2b). This behavior has important applications for this material in various industries such as chemistry, plastic, food, and drug.

Current study shows that XLG/AMPS hydrogels exhibit shear-thinning behavior, which means their viscosity decreases as the shear rate or applied stress increases. This property is advantageous for various applications as it allows for easy processing, injection, and spreading of hydrogel. The shear-thinning behavior arises from the disruption of the physical entanglements within the hydrogel network under shear stress. As the shear rate increases, XLG nanoparticles and polymer chains align and slide past each other, leading to a decrease in resistance to flow. Upon the removal of the shear stress, the hydrogel recovers its original viscosity, exhibiting a reversible shear-thinning behavior. The thixotropic behavior arises from the reversible breakdown and reformation of physical interactions within the hydrogel

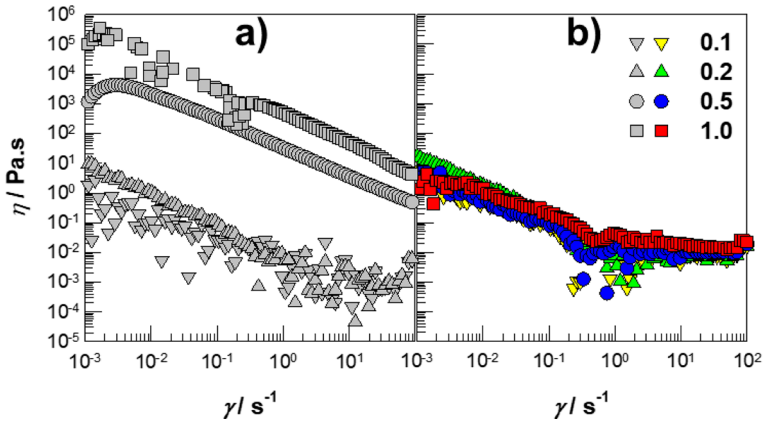

Fig. 2 **a, b:** Viscosity (η) of XLG dispersions in distilled water (**a**) and AMPS solutions (**b**). The amount of XLG dissolved in 10 mL of water is shown on the graph

network. Continuous agitation disrupts the physical entanglements between the XLG nanoparticles and polymer chains, resulting in a decrease in viscosity. Once the agitation ceases, the hydrogel gradually rebuilds its network structure, leading to the recovery of viscosity over time.

Figure S1a and b demonstrates that the samples have a gel state of up to 0.1 g mL^{-1} without AMPS, but with AMPS, they become a highly distributed solution of up to 0.2 g mL^{-1}. This increase in dispersability allows for higher concentrations of the sample and greater efficiency in the extraction process. The addition of AMPS also improves the viscosity of the sample, creating a more uniform solution. This in turn allows for more precise and accurate measurements of the sample. Additionally, the increased viscosity also improves the stability of the sample, allowing for better preservation of the sample over time.

The increasement in XLG concentration does not change the frequency dependence of the dynamic system (Fig. 3). This frequency dependence is due to the ability of XLG to absorb energy and dissipate it as heat. This property enables XLG to change the dynamic behavior of the system, resulting in higher efficiency in the energy transfer process. This significantly reduces the energy loss in the system, resulting in improved performance and efficiency. It makes XLG an ideal material for energy transfer applications, as its properties can be tailored to accommodate specific processes.

In Fig. 3, the loss factor δ decreased as XLG concentration increased, indicating increased crosslinking but no stacking or precipitation. The results suggest that XLG can be used to control the rheological properties of the system without compromising product stability. Furthermore, the addition of XLG had no significant impact on the viscosity of the system. It is extensively diffused and acts as a macro-crosslinker. XLG is a suitable stabilizer for these systems, providing beneficial rheology modifications without increasing viscosity and improved stability and rheological properties. Additionally, XLG/AMPS compounds reduce swelling effects as well. This results in a significant improvement in the physical and chemical properties of the formulation. XLG also enables the formulation of products with improved shelf life and longer product stability.

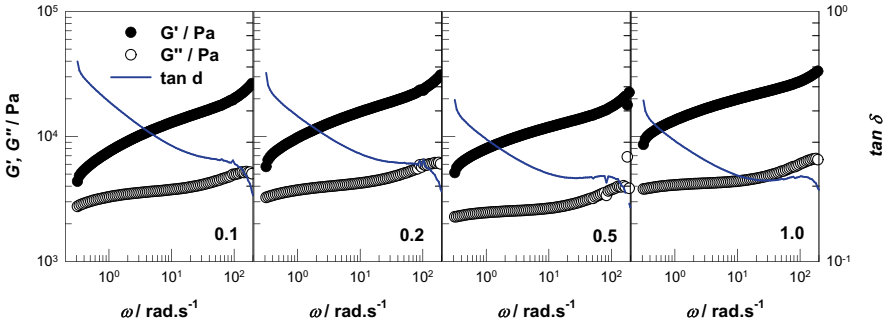

Fig. 3 Frequency sweep tests of XLG/AMPS hydrogels. XLG content is given on graphs. Elastic G' (filled), viscous modulus G'' (open symbols), and loss factor δ (lines) were drawn according to angular frequency ω. The amount of XLG dissolved in 10 mL of water is shown on the graph

Overall, XLG nanoparticles interact with the polymer chains through electrostatic interactions, hydrogen bonds, and van der Waals forces. These interactions promote stronger interfacial adhesion and improved stress transfer between the nanoparticles and the polymer matrix, resulting in enhanced mechanical properties. By incorporating XLG nanoparticles into the hydrogel, a tortuous path is formed for water or solute diffusion.This diffusion increases the resistance of the gels to swelling and helps maintain its structural integrity under mechanical stress. The layered structure of XLG provides a reinforcing effect, improving the hardness and structural integrity of the gels. The mechanical properties of the resulting hydrogel were increased by varying upward the concentration of XLG nanoparticles. Increasing the nanoparticle concentration generally leads to improved mechanical strength and stiffness, up to a certain threshold where excessive nanoparticle loading may compromise the integrity of gels. Surface modifications of XLG nanoparticles can be employed to enhance their compatibility with the AMPS system. By functionalizing the nanoparticle surface and adding AMPS polymer chains with affinity to the nanoparticle surface, stronger interactions were achieved, leading to improved mechanical properties. XLG/AMPS hydrogels possess a high-water absorption capacity due to the hydrophilic nature of AMPS monomers. The presence of XLG nanoparticles within the hydrogel network can modulate the swelling behavior, allowing for the control of gel properties and release kinetics. The results for a 0.5 w/v AMPS solution show that the addition of a large amount of AMPS property is prominent, and it is brittle in the swelling stage (Figure S2).

Ternary systems

Although the mechanical properties at after-synthesis conditions are promising for the AMPS/XLG system, the values of the swollen samples are limited due to the high swelling capacity of AMPS. Although the first method that comes to mind to correct this is to reduce the AMPS content or increase the chemical crosslink ratio, these applications will affect the dispersion of Laponite (XLG) or cause the hydrogel to turn into conventional brittle gels. In these conditions, MAPTAC, a cationic monomer, was included in the structure to limit the swelling of AMPS and increase the effect of reversible bonds in the structure. Similarly, an aqueous solution of anionic and cationic monomers was prepared and XLG was added to it with a maximum concentration of 0.2 g mL^{-1}, and the chemical crosslinker ratio was kept constant as 1/80 compared to the total monomer mole. The equilibrium swelling ratios by mass $m_{rel,eq}$ of the hydrogels obtained as a result of photopolymerization of the solution in which XLG is distributed homogeneously cannot exceed 1.5. Thus, tough materials that are not brittle even when they have reached swelling equilibrium in water can be produced, and the degree of essential chemical crosslinking and strain sensitivity is not compromised. The ionic bonds between anionic and cationic monomers were strengthened by entanglements, and the targeted mechanical properties were achieved.

In the second set of experiments in which the ternary system was examined, the swelling degree of XLG-PAM hydrogels prepared at equimolar concentrations

by mass and volume after synthesis was monitored for 10 days. The hydrogels in all XLG contents reached swelling equilibrium in distilled water within 48 h (Figure S3). At equilibrium swelling ratio by mass $m_{rel,eq}$ and volume $V_{rel,eq}$ is plotted against the XLG content, indicating the magnitude of the interaction with increasing XLG amount and decreasing degree of swelling (Figure S3b).

The stress–strain curves of XLG-PAM ternary systems obtained under compression tests and the mechanical parameters such as toughness W, modulus E, fracture stress σ_f, and strain ε_f % calculated as a result of these measurements are summarized in Figs. 4 and 5 for samples that swollen and after preparation states (Table 1).

To examine the ternary system in detail, cylindrical samples were subjected to compressive deformation at different strain rates $\dot{\varepsilon}$. XLG-PAM hydrogels show strain sensitive mechanical properties owing to their dominant physical crosslinked nature. Figure 6 a and b shows the stress–strain curves measured in the range of 10^{-3}–10^{-1} s^{-1} strain rate $\dot{\varepsilon}$ for samples in the after preparation and swollen states, respectively. Figure 6c shows the fracture stress varying depending on the strain rate $\dot{\varepsilon}$. For both after preparation (filled symbols) and swollen samples (open symbols), the fracture stress is directly proportional to the logarithmic strain rate in $\dot{\varepsilon}$. Young's modulus E and ftacture stress σ_f values are shown in Fig. 6d–g with horizontal columns. Filled columns belong to after preparation samples, and open columns belong to swollen samples.

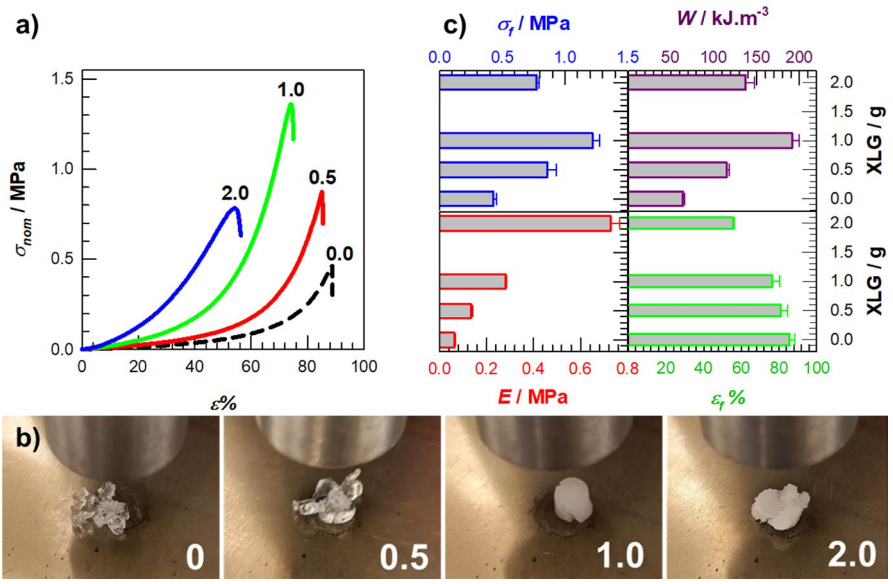

Fig. 4 **a** Stress–strain curves for XLG-PAM hydrogel samples (solid lines) at after-preparation states. Dashed line refers to PAM hydrogel prepared without XLG. **b** Images of fractured samples after 90% compression. **c** Mechanical parameters obtained from compression tests of samples according to XLG content. The amount of XLG dissolved in 10 mL of water is shown on the graph

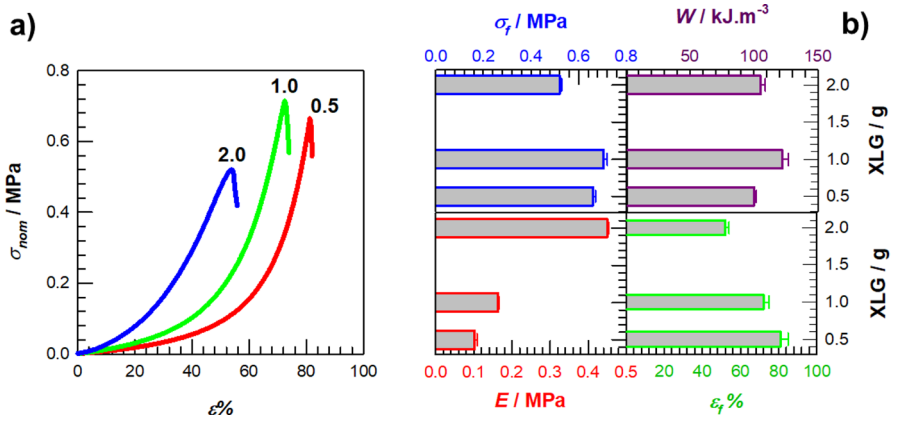

Fig. 5 **a** Stress–strain curves for XLG-PAM hydrogel samples (lines) at swollen states. The amount of XLG dissolved in 10 mL of water is shown on the graph. **b** Mechanical parameters obtained from compression tests of samples according to XLG content

Table 1 Mechanical parameters of samples at after-preparation and swollen states

Sample	XLG/g	*E*/kPa	σ_f/kPa	ε_f %	*W*/kJ m^{-3}	State
XLG-PA-1	1	219 (14)	5458 (35)	83	665 (39)	After prep.
XLG-PA-2	2	1238 (76)	1295 (89)	48	222 (17)	
XLG-PAM-1	1	282 (4)	1222 (53)	76	192 (8)	
XLG-PAM-2	2	728 (37)	775 (17)	56	138 (10)	
XLG-PA-1	1	1000 (88)	620 (4)	47	49 (2)	Swollen
XLG-PA-2	2	478 (12)	340 (22)	45	424 (9)	
XLG-PAM-1	1	163 (4)	705 (15)	72	122 (5)	
XLG-PAM-2	2	450 (4)	520 (9)	52	105 (4)	

Young modulus = *E*, fracture stress = σ_f, fracture strain = ε_f % and toughness = *W*. Standart deviations are given in parenthesis and they are smaller than 5% for ε_f %

Conclusion

The physical interactions between Laponite (XLG) and AMPS hold a fascinating interplay of ionic interactions and chemical structure, resulting in drastic effects that have profound implications for advanced applications. The platelet-like morphology of XLG provides a reinforcing effect, improving the mechanical strength, stiffness, and dimensional stability of the gels. The interactions between the sulfonic acid groups of AMPS and the polymer chains contribute to enhanced interfacial adhesion and compatibility, resulting in reduced permeability to gases and liquids. These effects have significant implications for a wide spectrum of applications. Controlled drug release systems can harness the gel-like structure to control the release of drugs, offering improved therapeutic efficacy and reduced side effects. Coatings and adhesives can benefit from the thixotropic behavior and

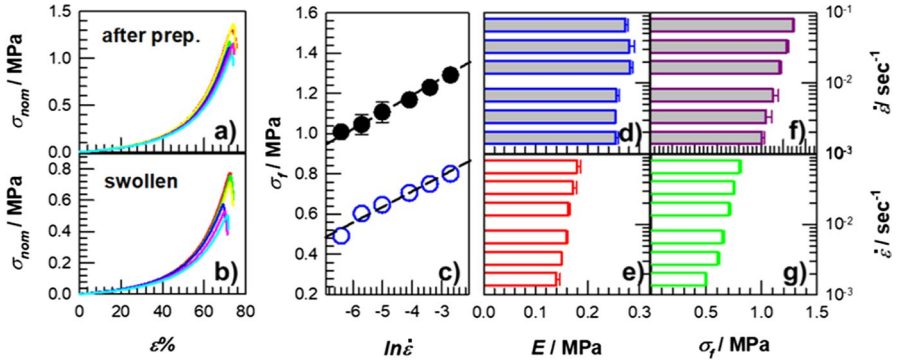

Fig. 6 **a, b:** Stress–strain curves depending on compression rate $\dot{\epsilon}$ of the samples after preparation (**a**) and swollen state (**b**). **c:** Fracture stresses σ_f of the XLG-PAM-1 hydrogel after preparation (filled symbols) and swollen state (open symbols) depending on the strain rate ln $\dot{\epsilon}$. **d–g:** Young's moduli E and fracture stresses σ_f of samples at after-preparation (**d**, **f**) and swollen states (**e**, **g**) calculated at different compression rates (horizontal bars)

enhanced mechanical properties of binary systems, enabling structural stability, easy application, and robust bonding. Additionally, the development of high-performance barrier materials for packaging, membranes, and protective coatings can be achieved using XLG-PA composites. On the other hand, XLG-PAM ternary systems dominated by reversible physical crosslinks are strain rate sensitive materials. Here, the change in mechanical properties of gels subjected to compression deformation at strain rate $\dot{\epsilon}$ of 10^{-3}–10^{-1} s^{-1} was investigated. This study provides insight into how to create strong supramolecular hydrogels with physical crosslinks that have improved mechanical properties that are strain rate dependent.

Experimental

Materials

Silicic acid, lithium magnesium sodium salt commercially name as Laponite XLG ($Li_{0.66}Mg_{5.34}Si_8O_{20}(OH)_4Na_{0.66}$; 53320-86-8) provided by Rockwood Additives Ltd. (UK). 2-Acrylamido-2-methyl-1-propanesulfonic acid ($H_2C=CHCONHC(CH_3)_2CH_2SO_3H$; 15214-89-8), [3-(Methacryloylamino) propyl]trimethylammonium chloride solution (50 wt% in H_2O; $H_2C=C(CH_3)CONH(CH_2)_3N(CH_3)_3Cl$; 51410-72-1), *N*,*N*′-Methylenebis(acrylamide) ($(H_2C=CHCONH)_2CH_2$; 110–26-9), and 2-Hydroxy-4′-(2-hydroxyethoxy)-2-methylpropiophenone commercially name as Irgacure 2959 ($HOCH_2CH_2OC_6H_4COC(CH_3)_2OH$; 106797-53-9) were purchased from Sigma-Aldrich (USA).

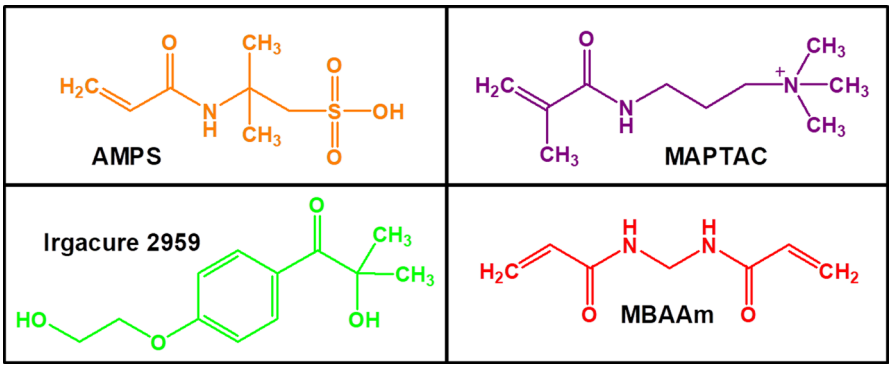

Hydrogel synthesis and swelling tests

All hydrogels, whether in binary or ternary system, were synthesized by the photopolymerization method using Irgacure 2959 (0.2 mol% respect to monomers), in a UV reactor equipped with 12 lamps at 360 nm wavelength, and after a reaction lasting 24 h at room temperature (25 ± 2 °C) controlled by a fan. In our experiments, AMPS or AMPS + MAPTAC total monomer concentration set at a constant 0.5 g mL^{-1}. This value is the water solubility limit of AMPS reported in our previous studies [19, 24]. In addition, in all experiments, *N*,*N*′-Methylenebis(acrylamide), MBAAm was used as a chemical crosslinker at a ratio of 1/80 mol based on the total monomer amount $(n_{MBAA})/n_{AMPS}$ and/or $(n_{MBAA})/n_{AMPS} + n_{MAPTAC}) = 1/80$. Within the scope of the study, the experiments were carried out in two sets as double and triple systems. The first set of experiments involves creating hydrogels from a solution made by combining 5 g of AMPS and 0.1–2 g of Laponite (XLG) in 10 mL of deionized water. The second set includes the solution prepared by dissolving 0.1–2 g XLG and 2.5 g AMPS and 5 g MAPTAC solution (50% by weight in water) in 7.5 mL distilled water and the hydrogels prepared from them. Solutions prepared by dissolving 0.1–1 g XLG in 10 mL distilled water were used as control for both sets of experiments. Control sample containing 2 g XLG could not be prepared due to the aggregation and solubility problem of XLG. The amounts of XLG, monomer, and water employed in the synthesis are compiled in Table S1. For example, for the synthesis of ternary hydrogel (*XLG-PAM-1*) containing 1 g of XLG, AMPS (2.5 g, 12 mmol), and MAPTAC (5 g, 11 mmol) are dissolved in water. Then, MBAAm (0.04 g, 0.29 mmol) is added to solution, after 5 min of stirring the mixture under nitrogen bubbling, it was slowly mixed until a homogeneous solution was formed and the photoinitiator Irgacure 2959 (0.01 g, 0.05 mmol) was added to the solution. Without waiting, the solution was transferred to 1 mL syringes, and the polymerization was continued for 24 h in the UV reactor.

The hydrogels were removed from the syringes after synthesis were cut into 10-mm lengths for water-swelling tests. Cylindrical samples with a diameter of

4.6 mm were immersed in deionized water at 25 ± 2 °C and the water was refreshed daily. The mass and diameter of the samples were followed for 10 days. The samples, which reached swelling equilibrium, extracted from the water and were placed to the freeze dryer (Christ Alpha 2e4 LD-plus) to be dried. The degree of swelling in equilibrium by weight $m_{rel,eq}$ and volume $V_{rel,eq}$ was calculated with the following equations.

$$m_{rel,eq} = m/m_0 \tag{1}$$

$$V_{rel,eq} = d^3/d_0^3 \tag{2}$$

While m_0 and d_0 in the expression are the mass and diameter for the samples after synthesis, m and d are the values of the samples reaching the swelling equilibrium.

Rheological and mechanical measurements

The rheological properties of XLG solutions (control group), binary (XLG/AMPS), and ternary (XLG/AMPS/MAPTAC) systems were investigated with the Gemini 150 rheometer system in which temperature control is carried out with a peltier (Bohlin Instruments). The viscosities η of the control group, binary, and ternary system solutions were measured using a cone-and-plate geometry, the cone is 40 mm in diameter, with a cone angle of 4° in a range of shear rates between 10^{-3} and 10^{2} s^{-1}. The strain amplitude γ_0 in frequency sweeps where frequency dependent elastic G', viscous modulus G',$'$ and loss factor δ are measured is 0.1. The mechanical properties of the binary and triple hydrogels were measured with a uniaxial mechanical testing machine (Zwick Roell Z0.5 TH) equipped with a 500 N load cell at 25 ± 2 °C. Cylindrical specimens with a diameter of 4.6 mm and a length of 5 mm were subjected to uniaxial compression tests. Measurements are presented in the form of nominal stress σ_{nom} vs. strain ε. The nominal stress σ_{nom} is the force applied per cross-sectional area of the undeformed gel specimen, while the strain ε is the ratio of the initial length of the gel sample to the amount of deformation. Mechanical parameters such as Young's modulus E and toughness W of the specimens are calculated from the slopes of the stress–strain curves in the linear region (5–15% region of the strain) and the area under these curves, respectively.

Supplementary Information The online version contains supplementary material available at https://doi.org/10.1007/s00289-024-05171-7.

Acknowledgements This work was supported by the Science Committee of the Ministry of Science and Higher Education of the Republic of Kazakhstan (IRN AP23489409). Authors thank to Polymeric Gel Research Lab. (ITU/Polymer) for measurements.

Author contributions G.T. and E.S. contributed to the conceptualization; G.T. and E.S. were involved in the methodology; G.T. and G.Y. assisted in the investigation; G.T. contributed to the resources; G.T. and G.Y. were involved in the data curation; G.T. assisted in the writing—original draft preparation; E.S. contributed to the writing—review and editing; E.S. was involved in the visualization; and G.T. assisted in the project administration; G.T was involved in the funding acquisition. All authors have read and agreed to the published version of the manuscript.

Funding Open access funding provided by the Scientific and Technological Research Council of Türkiye (TÜBİTAK).

Availability of data and materials Not applicable.

Declarations

Conflict of interest The authors declare no conflicts of interests.

Ethical approval Not applicable.

References

1. Abdurrahmanoglu S, Okay O (2010) Rheological behavior of polymer-clay nanocomposite hydrogels: effect of nanoscale interactions. J Appl Polym Sci 116(4):2328–2335. https://doi.org/10.1002/app.31705
2. Buyukbektas A, Delibas A, Benk A, Coskun R (2021) Laponite-AMPS/AA composite hydrogels for efficient removal of methylene blue (MB). J Polym Res. https://doi.org/10.1007/s10965-021-02677-w
3. Campbell D, Tighe BJ (2008) Zwitterionic and charge-balanced polyampholyte copolymer hydrogels. In: Tunkasiri T (ed) Smart materials. Adv Mater Res, vol 55–57, pp 729–732. https://doi.org/10.4028/www.scientific.net/AMR.55-57.729
4. Davila JL, d'Avila MA (2019) Rheological evaluation of Laponite/alginate inks for 3D extrusion-based printing. Int J Adv Manuf Technol 101(1–4):675–686. https://doi.org/10.1007/s00170-018-2876-y
5. Jain M, Matsumura K (2016) Polyampholyte- and nanosilicate-based soft bionanocomposites with tailorable mechanical and cell adhesion properties. J Biomed Mater Res A 104(6):1379–1386. https://doi.org/10.1002/jbm.a.35672
6. Kudaibergenov SE, Ciferri A (2007) Natural and synthetic polyampholytes, 2(a) functions and applications. Macromol Rapid Commun 28(20):1969–1986. https://doi.org/10.1002/marc.200700162
7. Kudaibergenov SE (2019) Physicochemical complexation and catalytic properties of polyampholyte cryogels. Gels. https://doi.org/10.3390/gels5010008
8. Li GH, Ji XX, Sun JH, Yuan ZW, Wang YX (2018) Mechanical and self-healing properties of poly acrylic acid/Laponite/Fe3+ nanocomposite hydrogel. Sci Adv Mater 10(12):1813–1822. https://doi.org/10.1166/sam.2018.3402
9. Ladika M, Kalantar TH, Shao H, Dean SL, Harris JK, Sheskey PJ, Coppens K, Balwinski KM, Holbrook DL (2014) Polyampholyte acrylic latexes for tablet coating applications. J Appl Polym Sci. https://doi.org/10.1002/app.40049
10. Li J, Tian ZH, Yang H, Duan L, Liu YF (2023) Infiltration of laponite: an effective approach to improve the mechanical properties and thermostability of collagen hydrogel. J Appl Polym Sci. https://doi.org/10.1002/app.53366
11. Li YX, Zhao DL, Wang ZY, Meng YL, Liu BH, Li L, Liu R, Dong SC, Wei FL (2023) Minimally invasive bone augmentation through subperiosteal injectable hydroxylapatite/laponite/alginate nanocomposite hydrogels. Int J Biol Macromol. https://doi.org/10.1016/j.ijbiomac.2023.123232

12. Lin L, Luo YH, Li X (2019) Synthesis of diblock polyampholyte PAMPS-b-PMAPTAC and its adsorption on bentonite. Polymer. https://doi.org/10.3390/polym11010049
13. Mourchid A, Levitz P (1998) Long-term gelation of laponite aqueous dispersions. Phys Rev E 57(5):4887–4890. https://doi.org/10.1103/PhysRevE.57.R4887
14. Okay O, Durmaz S (2002) Charge density dependence of elastic modulus of strong polyelectrolyte hydrogels. Polymer 43(4):1215–1221. https://doi.org/10.1016/s0032-3861(01)00723-6
15. Okay O, Sariisik SB, Zor SD (1998) Swelling behavior of anionic acrylamide-based hydrogels in aqueous salt solutions: comparison of experiment with theory. J Appl Polym Sci 70(3):567–575. https://doi.org/10.1002/(sici)1097-4628(19981017)70:3%3c567::aid-app19%3e3.0.co;2-y
16. Pacelli S, Paolicelli P, Moretti G, Petralito S, Di Giacomo S, Vitalone A, Casadei MA (2016) Gellan gum methacrylate and laponite as an innovative nanocomposite hydrogel for biomedical applications. Eur Polym J 77:114–123. https://doi.org/10.1016/j.eurpolymj.2016.02.007
17. Pojanavaraphan T, Liu L, Ceylan D, Okay O, Magaraphan R, Schiraldi DA (2011) Solution cross-linked natural rubber (NR)/clay aerogel composites. Macromolecules 44(4):923–931. https://doi.org/10.1021/ma102443k
18. Ruzicka B, Zulian L, Ruocco G (2007) Ageing dynamics in Laponite dispersions at various salt concentrations. Philos Mag 87(3–5):449–458. https://doi.org/10.1080/14786430600962732
19. Sekizkardes B, Su E, Okay O (2023) Mechanically strong superabsorbent terpolymer hydrogels based on AMPS via hydrogen-bonding interactions. ACS Appl Polym Mater 5:2043–2050. https://doi.org/10.1021/acsapm.2c02085
20. Shukla NB, Madras G (2011) Reversible swelling/deswelling characteristics of ethylene glycol dimethacrylate cross-linked poly(acrylic acid-co-sodium acrylate-co-acrylamide) superabsorbents. Ind Eng Chem Res 50(19):10918–10927. https://doi.org/10.1021/le200713y
21. Su E, Okay O (2019) Cryogenic formation-structure-property relationships of poly(2-acrylamido-2-methyl-1-propanesulfonic acid) cryogels. Polymer. https://doi.org/10.1016/j.polymer.2019.121603
22. Su E, Okay O (2018) Hybrid cross-linked poly(2-acrylamido-2-methyl-1-propanesulfonic acid) hydrogels with tunable viscoelastic, mechanical and self-healing properties. React Funct Polym 123:70–79. https://doi.org/10.1016/j.reactfunctpolym.2017.12.009
23. Su E, Okay O (2017) Polyampholyte hydrogels formed via electrostatic and hydrophobic interactions. Eur Polym J 88:191–204. https://doi.org/10.1016/j.eurpolymj.2017.01.029
24. Su E, Yurtsever M, Okay O (2019) A self-healing and highly stretchable polyelectrolyte hydrogel via cooperative hydrogen bonding as a superabsorbent polymer. Macromolecules 52(9):3257–3267. https://doi.org/10.1021/acs.macromol.9b00032
25. Toleutay G, Shakhvorostov AV, Kabdrakhmanova SK, Kudaibergenov SE (2019) Solution behavior of quenched or strongly charged polyampholytes in aqueous-salt solutions. Bull Karaganda Univ Chem Ser 94:5–44. https://doi.org/10.31489/2019Ch2/35-44
26. Toleutay G, Su E, Kudaibergenov SE (2019) Swelling and mechanical properties of quenched polyampholyte hydrogels based on 2-acrylamido-2-methyl-1-propanesulfonic acid sodium salt (AMPS) and (3-acrylamidopropyl) trimethylammonium chloride (APTAC). Bull Karaganda Univ Chem Ser. 96:35–43. https://doi.org/10.31489/2019Ch4/35-43
27. Toleutay G, Su E, Kudaibergenov S, Okay O (2020) Highly stretchable and thermally healable polyampholyte hydrogels via hydrophobic modification. Colloid Polym Sci 298(3):273–284. https://doi.org/10.1007/s00396-020-04605-8
28. Uzumcu AT, Guney O, Okay O (2016) Nanocomposite DNA hydrogels with temperature sensitivity. Polymer 100:169–178. https://doi.org/10.1016/j.polymer.2016.08.041
29. Valle H, Sanchez J, Rivas BL (2015) Poly(N-vinylpyrrolidone-co-2-acrylamido-2-methylpropanesulfonate sodium): synthesis, characterization, and its potential application for the removal of metal ions from aqueous solution. J Appl Polym Sci 132(2):7. https://doi.org/10.1002/app.41272
30. Zhang TC, Ge JJ, Wu H, Guo HB, Jiao BL, Qian Z (2022) Effect of AMPS(2-acrylamido-2-methylpropane sulfonic acid) content on the properties of polymer gels. Pet Sci 19(2):697–706. https://doi.org/10.1016/j.petsci.2022.01.006